MATHMATICAL MODELING OF MASS TRANSFER FROM AN IMMERSED BODY TO A FLUIDIZED GAS BED

Zainab Talib Abidzaid al-Sharify
Al-Mustansiryiah University/College of Engineering
Environmental Engineering Department
Iraq - Baghdad /Bab-AL- Muthem/P.O. Box 14150
Zainab_talib2009@yahoo.com

Abstract:

Fluidization process is widely used by a great assortment of industries worldwide; one of these processes is the mass transfer from an immersed body to a fluidized gas bed. This work presents an experimental study of a continuous gas-solid fluidized bed with a porous material placed at the bottom of the column to support the packing material. Sand-air-naphthalene system has been used in this work. Sand with sizes distributed between 75-250 microns was used as solid fluidizing particles and air was used for fluidization in a 70 cm height and 8 cm inside diameter fluidization Column. Naphthalene was selected for this study as the immersed object, this have been done by making a spheres of wood of 2.9 cm outside diameter and coating this spheres wood with Naphthalene by dipping this spheres into a bath of molten naphthalene (at about 90^0C). An empirical correlation was developed for mass transfer of naphthalene vapor into air-sand fluidized bed by using experimental data of many variables such as temperature, air velocity, and sand particle size. The experimental results of the mass transfer in the present work have been compared in curve in Yokota's coordinate with many documented experimental literatures data. The comparison gave a very good agreement, and show that Sherwood number increased slowly with the increase in gas velocity at constant surface temperature and particle size.

Key Words: fluidization, mass transfer, sand-air-naphthalene system, Ziegler equation, Sherwood number, minimum fluidizing velocity, mass transfer coefficients.

النمذجة الرياضية لإنتقال المادة من جسم غاطس الى طبقة غازية مميعة

زينب طالب عبدزيد الشريفي
الجامعة المستنصرية كلية الهندسة قسم هندسة البيئة

الملخص:

ان عملية التميع واسعة الاستعمال في الصناعات العالمية المتعددة واحدة من هذه العمليات هي انتقال المادة من جسم غاطس الى طبقة غازية مميعة. ان هذا العمل يقدم دراسة تجريبية للتميع المستمر لنظام الغاز – الصلب مع مادة مسامية وضعت في أسفل العمود لدعم مواد الحشوة. تم في هذا العمل استخدام نظام رمل–هواء–نفثالين .ان الرمل المستعمل كجسيمات الصلب المتميع استخدم بأحجام مختلفة تتراوح بين ٧٥– ٢٥٠ مايكرون، ان سائل التميع كان الهواء. تم استخدام عمود تميع زجاجي بأرتفاع 70 سم وبقطر داخلي 8 سم. تم في هذه الدراسة استخدام المادة المغمورة وهي النفثالين، حيث تم طلاء كرات خشبية قطرها الخارجي ٢.٩ سم وذلك بإنزال هذه الكرات في حمام النفثالين المنصهر بدرجة حرارة حوالي ٩٠ درجة سليزية. تم تطوير

علاقة رياضية تربط معامل إنتقال المادة لبخار النفثالين الى الطبقة الغازية المميعة من الهواء والرمل، وذلك بدراسة العملية لعدة متغيرات كدرجة حرارة السطح ،معدل جريان الهواء وحجم الدقائق. ان النتائج التجريبية لأنتقال المادة في العمل الحالي تمت مقارنتها مع التجارب العملية الموثقة علميا. وهذه المقارنة اظهرت مطابقة جيدة جدا، وتم وضعها في رسومات على احداثيات يوكوتاس، حيث تم ايجاد ان رقم شيروود يتزايد ببطء مع زيادة سرعة الغاز بثبوت حرارة السطح والجسيمات.

Notations

Symbols		*Notations*	*Units*
C_s	=	Concentration at the surface.	mole /m^3
C_b	=	Bulk concentration.	mole / m^3
C_m , $\bar{C}_m$	=	Relative and mean relative mass capacity respectively	
C_{mf} ,C_{ms}	=	Specific mass capacity of gas and particles respectively	kg / kg
D_f	=	Molecular diffusivity in a gas	m^2 / s
D_s , $\bar{D}_s$	=	Effective and mean effective diffusivity in a particle respectively	m^2 / s
D_v, D_{v0}	=	Diffusivity of transferable component and at 0^0C respectively.	m^2 /s
d	=	Diameter of the bed.	m
d_p	=	Fluidizing particle diameter.	m
g	=	Gravitational force.	m/s^2
G	=	Gas mass velocity.	kg /m^2. s
G_{mf}	=	Gas mass minimum velocity.	kg /m^2. s
k_y'	=	Surface-to-inert bed mass transfer coefficient	kg / m^2.s
k_{yb}'	=	Surface-to-bubble mass transfer coefficient	kg / m^2.s
k_{yp}	=	Surface-to-packet mass transfer coefficient	kg / m^2.s
k_{yp}'	=	Surface-to-packet mass transfer coefficient for C_{ms}=0	kg / m^2.s
kg	=	Mass transfer coefficient.	m/s
L	=	Length of the column	m
m_s	=	Particle mass $m_s = \pi d_s^3 \rho_s / 6$	kg
M_s	=	Mass capacity of particles	m^3 / kg
N	=	Total surface-to-bed mass flux	kg/m^2.s
ΔP	=	Bed pressure drop.	mm Hg
P_s	=	Saturation partial pressure.	mm Hg
Re_p	=	Reynolds number based on the diameter of the inert particles.	-
R_{mp}, R_{mw}	=	Mass transfer packet and contact resistance respectively	m^2. s /kg
Sh	=	Sherwood number. $k_g d_s / D_v$	-
Sh_e	=	Sherwood number in empty bed.	-
Sh_p	=	Sherwood number in packet bed.	-
T	=	Temperature	^{0}C
T_s	=	Saturation partial temperature.	^{0}C
U_{mf}	=	Minimum fluidizing velocity.	m/s
U	=	Gas velocity	m/s
Y	=	Concentration of gas (mass of transferred substance per unit mass of inert gas)	kg/kg

Greek Letters

μ	=	Viscosity	kg/ s.m
μ_o	=	Viscosity of air at ^{0}C	kg/ s.m
ρ	=	Gas density.	kg/m^3
ρ_p	=	Particle density.	kg/m^3
ρ_f , ρ_s	=	Gas and solid density respectively	kg/m^3
ψ	=	Sphericity.	-
τ	=	Time	s
τ_b, $\bar{\tau}_b$	=	Bubble residence contact time and its mean value respectively	s

$\tau_p, \bar{\tau}_p$	=	Packet residence contact time and its mean value respectively	s
ε	=	Porosity	-
ε_p	=	Packet porosity	-

Subscripts

b	Bubble
f	Gas
m	Mass (minimum)
p	packet
s	Solid(particle)

Introduction:

Fluidized beds are commonly employed in chemical, biochemical and petrochemical industries in processes such as hydrocarbon cracking, drying of solid particles, combustion and gasification of coal and biomass, synthesis reactions and coating of particles. Gas-solid fluidized systems are characterized by temperature uniformity and high heat transfer coefficient due to the intense mixture of the solid material with the gas bubbles normally present (Pécora and Parise, 2006).

A number of correlations for mass transfer in fluidized beds have been proposed, most of these involve a single-line relationship between Reynolds number and the product of Sherwood number by some power of Schmidt number (Wankhede, 2009). **Resnick** (Resnick, 1949) calculated the mass transfer coefficient of naphthalene crystals of five different sizes ranged from 250 to 1000 microns in air, hydrogen, and carbon dioxide at a temperature of 298K and rates between 0.01 and 1.5 kg/m^2.s. **Gamson** (Gamson, 1951) utilized the available mass transfer data for packed and fluidized beds related the mass transfer modulus to the modified Reynolds group. **Gupta** and **Thosad** (Gupta and Thosad, 1962) correlated the mass transfer factor with the conventional Reynolds number utilizing all the available data. **Markova** and **Martyushin** (Markova and Martyushin, 1965) studied the effect of fluidized particle size on mass transfer coefficient with particle diameter of 0.565, 0.488 and 0.347 mm. They concluded that the increasing air velocity increases the mass transfer coefficient. **Shirai** (Shirai, et al., 1966) studied heat and mass transfer between fluidized bed and surface of single sphere fixed in the bed. Sand was employed as fluidizing particles for mass transfer study and the solid sphere was made of brick and the system used is air-water system. They found that the value of Sherwood number is only 1.5 times that for mass transfer between particles and fluid. **Ziegler** and **Holmes** (Ziegler and Holmes, 1966) studied mass transfer from fixed surface to gas fluidized beds. Mass transfer coefficients were measured for the diffusion of water vapor from a saturated porous sphere into various air-fluidized beds of solid particles. Naphthalene diffusion from coated flat plate into fluidized beds was also studied. **Gunn** (Gunn, 1987) studied the mass transfer in gas-solid fixed and fluidized beds operated in a wide range of velocities and porosities. He developed a theoretical correlation that expresses the mass transfer between the particles and fluids processes. **Kaneko** (Kaneko et al., 1999), **Rhodes** (Rhodes et al., 2001) and **Kafui (**Kafui et al., 2002) studied the general characteristics of a fluidized bed, such as the gradual change in particle characteristics and size distribution in the bed, and also studied the impact of inter particle forces on fluidization. **Schmidt** and **Renz** (Schmidt and Renz, 2005) investigate numerical analysis of the heat transfer between fluidized bed of mono-dispersed glass beads and an immersed heater tube. An **Eulerian** approach has been used for the solution of the mass, momentum and energy equations of both phases. **Pécora** and **Parise** (Pécora and Parise, 2006) presents an experimental study of a continuous gas-solid fluidized bed with an immersed horizontal tube. Silica sand of 254μm diameter was used as solid particles and air was used for fluidization in a 900mm long and 150mm wide heat exchanger. An empirical correlation for the heat transfer coefficient was proposed as a function of solid particle and gas mass flow rate, number of baffles and gas velocity. **Wankhede** (Wankhede, 2009) study the effect of surface temperature on average heat transfer coefficients in a sound assisted fluidized bed of fine powders. He found that for both coarse grained and fine particles, the heat transfer rates can be improved by increasing

the surface temperatures. He presents the data as a function of excess air velocity and sound pressure level.

The objective of this work is to:

1- Writing a mathematical model for mass transfer from an immersed body to a gas fluidized bed depending on variables affecting the mass transfer.
2- Study the effect of different factors on the gas-solid system, such as fluid properties, fluidized properties, and nature of the flow, as well as the effect of each one on the others.
3- Determine the dependence of mass transfer coefficient on fluidized bed variables. Many variables effect mass transfer have been investigated such as: air velocity, sphere surface temperature, size of fluidizing particles and sphere size.
4- Predicate the mass transfer coefficient from the knowledge of mass transfer coefficient in the absence of fluidizing particles, plus a term that describes the effect of fluidizing solid particles on transfer rate coefficients.

Minimum Fluidizing Velocity

When the gas is passed upwards through a fluidized bed unrestrained at its upper surface, the pressure drop increases with gas velocity increasing, the drag on an individual particle excess the force exerted by gravity. Then an excess pressure is required to free the particles that are interlocked at the fluidized state and theoretical pressure drop. The velocity at the point that the pressure drop falls back is called the minimum fluidizing velocity (U_{mf}) (Gupta and Sathiyamoorthy, 1999). **Leva** (Leva et al., 1951) worked with round and sharp sands of 0.05-0.40 mm using 0.1 m diameter with various depths fluidized by air. He noted that the smaller particles require an extra of energy for fluidization. The **Wen** and **Yu** produced an empirical correlation for U_{mf} for gas fluidization. Wen and Yu (Wen and Yu, 1966) correlation is often taken as being most suitable for particles larger than 100 μm, whereas the correlation of **Baeyens** and **Geldart** (Baeyens and Geldart, 1974) is best for particles less than 100μm, which is shown in eq. 1:

$$U_{mf} = \frac{d_p^{1.8}(\rho_p - \rho)^{0.934} g^{0.934}}{110\mu^{0.87}\rho^{0.066}} \quad (1)$$

Model for Mass Transfer in Fluidized Bed

The process of mass transfer from an immersed body to a gas fluidized bed has not yet been intensively investigated. To describe the process mathematically **Baskakov** (Baskakov and Suprun, 1970) and **Prozorov** (Prozorov, 1976) assumed that mass is transmitted from the surface by packets of particles and by gas bubbles as follows:

$$k_{y'} = (1-f_o)k_{yp'} + f_o k_{yb'} \quad (2)$$

Where:

$$f_o = \frac{\bar{\tau}_b}{\bar{\tau}_b + \bar{\tau}_p} \quad (3)$$

In contrast to heat transfer theory where the heat within a packet is transferred through gas and particles and the accumulation of heat within particles plays a dominant role. These workers assumed that mass within a packet is transferred only by gas between particles occurs. Thus the mass transfer coefficient to a packet was found to be (Markova and Martyushin, 1965; Baskakov and Suprun, 1972; Baskakov et al., 1973):

$$k_{yp'} = 2\rho_f \left(\frac{D}{\pi\bar{\tau}_p}\right)^{1/2} \quad (4)$$

$$k_{yb'} = 2\rho_f \left(\frac{D_b}{\pi\bar{\tau}_b}\right)^{1/2} \quad (5)$$

It must be remembered that all the above considerations apply to an inert fluidized bed (Baskakov, 1974). If adsorption of a transported substance onto the particles takes place the mass transfer coefficient rises and the ratio (k_y/k_{yf}) may then reach values from 3 to 15 (Ziegler and Holmes, 1966). For such cases, on the basis of the packet theory and allowing for mass accumulation on particles, **Yokota** (Yokota et al., 1975) derived the following expression:

$$k_{yp} = \rho_f \left(\frac{\varepsilon_p D_f M_s \rho_s (1-\varepsilon_p)}{\bar{\tau}_p} \right)^{1/2} \quad (6)$$

Eq. 6 transformed into the dimensionless form, as shown below:

$$Sh_p = \left(\frac{\varepsilon_p (1-\varepsilon) M_s \rho_s L^2}{D_f \bar{\tau}_p} \right)^{1/2} \quad (7)$$

In this work the mass capacity process was investigated and described on the basis of the modified packet model including the mass contact resistance. For the contact resistance control region the alternative simplified packet model was developed. In order to derive the simplified packet model equations, two assumptions are made:

1- For sufficiently short packet contact times which correspond to vigorous fluidization and for relatively large particles, only the first layer of particles, i.e. those in contact with the surface, participate in surface-packet mass transfer.
2- During the time that a packet remains at the surface, a particle in the first layer adsorbed to the surface.

Dimensional Analysis:

The dimensionless group, *Y*, is a function of all the variables and dimensionless constant which take into account the influence of particles motions. These factors may be arranged in a suitable form of dimensional analysis using Buckingham's π theorem (Buckingham, 1914), such as:

$$Y = f(\psi, d_p, (\rho_p - \rho), \rho, \mu, (G - G_{mf}), g) \quad (8)$$

$$Y = [\psi d_p]^a [(\rho_p - \rho)\rho]^b [G - G_{mf}]^c g^d \mu^e \quad (9)$$

The common groups for mass transfer are Sherwood number, Schmidt number and Reynolds number. In Buckingham's π theorem, the dimensions of a physical quantity are associated with mass, length and time, represented by symbols m, L and θ respectively, each raised to rational powers. The number of dimensionless groups obtained from the dimensional analysis are equal to the number of variables, *n=5*, minus the number of fundamental dimensions, *r=3*, and hence two dimensionless groups will be obtained. In term of fundamental dimensions:

$$1 = [L]^a \left[\frac{m^2}{L^6}\right]^b \left[\frac{m}{L^2\theta}\right]^c \left[\frac{L}{\theta^2}\right]^d \left[\frac{m}{L\theta}\right]^e \quad (10)$$

From these results we obtain

$$Y = [\psi d_p]^{-e-b} [(\rho_p - \rho)\rho]^b [G - G_{mf}]^{-2b-e} [g]^b [\mu]^e \quad (11)$$

$$Y = \left[\frac{(\rho_p - \rho)\rho g (\psi d_p)}{(G - G_{mf})^2}\right]^b \left[\frac{(\psi d_p)(G - G_{mf})}{\mu}\right]^{-e} \quad (12)$$

From the above equation, one can notice that the first term is the invert of Froude number (*Fr*) and the second is the modified Reynolds number (*Re*).

Experimental Set-Up and Method

Sand-air-naphthalene system has been used in this work. Sand was employed as fluidizing particles, which can be regarded as a non-absorptive material. A sand bed material was employed in this investigation with three different particle sizes, with range of 75-250 micron, in order to get a smooth fluidization. The properties of sand particles used in this work are shown in **Table 1**. The immersed object used has a spherical shape of 2.9 cm outside diameter made of wood, which was coated with hard smooth surface of naphthalene. This was done by dipping the spheres into a bath of molten naphthalene at about 90°C. The immersed object was fixed in the center of the column by suspending it with a steel rod. The spherical shape was used in order to minimize the dead zone around the immersed object, and because spherical shapes have many applications in the industrial. A photographic picture of the apparatus used is shown in **Figure 1**.

The experimental system, as outlined in **Figure 2**, consists of the main components: fluidization column, air compressor, air flow meter, U-tube manometer, bed material (sand), immersed work piece, heating equipment (heating element, variac), and temperature measurement device. The *fluidization Column* was made of glass column (Q.V.F) 8 cm inside diameter and 70 cm height. A *porous material* was placed at the bottom of the column to support the packing material. *Air compressor* was used to supply air with a surge tank to store the air and minimize the fluctuation. An automatic regulator in the *compressor* was used to regulate the pressure of the air inside the tank. The amount of air which left the compressor was controlled by the use of the tank and valve. A *calibrated air flow meter* was used to measure the air flow rate which entered the column. The range of the air flow meter is 0-16 m^3/hr. The pressure drop across the bed was measured by the use of *U-tube manometer* which made of glass with total length of 0.75 m. The manometer was placed on a wide sheet of wood with a measuring tape for the measurement of the level difference of the liquid (water) inside the tube. An *electrical heater* placed inside 2" Q.V.F. glass tube has been used as the heating equipment. The variation in heat supplied from the heater was controlled by the use of a variac connected directly to the heater. Two *thermocouples* were used for temperature measurement; the thermocouples were located in two different locations in order to measure the temperature about 3 cm under and above the spheres. These thermocouples were connected to digital readers that show the value of temperature.

Experimental Procedure

The pressure drop of the bed was determined by subtracting the pressure drop of distributor from total pressure drop that are found for a range of superficial gas velocities after loading known weight of sand particles having known diameter into the bed to a static level of 30 cm. Curves of pressure drop across the bed versus superficial gas velocity are shown in **Figures 3, 4, 5** and **6**.

Mass transfer coefficient value in empty bed has been determined experimentally, by placing two thermocouples and other devices and connected them to the column. The compressor started blowing air into the tank until it reached the desired pressure to turn the compressor off by the automatic regulator. The tanks valve was turned on. The air flowed through the rotameter to the bed until rotameter read a constant desired value of the air flow rate. At the same time the heater was turned on for the desired power which was controlled by the use of the variac. The measurements of the pressure drop across the bed were made by the use of the U-manometer. When the conditions reach to steady state (constant flow rate and constant temperature), the coated sphere was lowered inside the column 15 cm above the distributor surface. Every 5 minutes, the sphere was taken out of the bed and the change of weight was measured by digital balance. This have been repeated for arrange of air superficial velocities and a range temperatures.

The Mass Transfer coefficient value from the sphere sand to the fluidized bed has been determined experimentally, by weighting a quantity of sand and poured it into the column from the top for a known and constant height of 30 cm for all runs carried in the work. Two thermocouples in their place were connected to the column. The compressor started blowing air into the tank until it reached the desired pressure to turn the compressor off by the automatic regulator. The tanks valve was turned on. The air flowed through the rotameter to the bed until rotameter read a constant desired value of the air flow rate. At the same time the heater was turned on for the desired power that was controlled by the use of the

variac. When conditions reach to steady state (constant flow rate and constant temperature); the coated sphere was lowered inside the column 15 cm above the distributor surface.

Results And Discussion:

A set of experiments at different air velocities and different temperatures were performed for mass transfer in empty bed (air stream only), to check the results with previous works. Operational conditions and experimental results for mass transfer coefficient for each experimental test are presented in **Table 2** and **4**. From **Table 4** it can be seen clearly that experiments were carried out at temperature below 70℃, to avoid naphthalene melting. A set of experiments were performed to determine the value of mass transfer coefficient from the sphere to the fluidized bed, the experimental conditions and results for this experiments are listed in **Table 3** and **5**. The air velocity is chosen to be within the range (1-1.4) U_{mf}, because this range of flow is usually used in industrial practice. The particle size of sand was selected to be as fine particles in order to get a smooth fluidization.

Correlations of the Experimental Results

Many variables are influence mass transfer coefficient such as diffusivity of the active component through the fluid, superficial flow rate of the fluid, density and viscosity of the fluid, and shape and size of the spaces between the particles in the bed. A number of assumptions were made to get accurate relationship of the variables influence on mass transfer coefficient:

1- Neglect the abrasion effects and assume the weight loss of naphthalene is mainly due to evaporation.
2- Void fraction of fluidizing sand particles equals the void fraction at minimum fluidizing velocity.
3- Partial pressure of naphthalene at the surface everywhere equal to the saturation partial pressure of vapor at the surface temperature of the solid sphere, the partial pressure of naphthalene at the bulk of air stream was equal to zero. Change in surface area of the sphere along the experiment was neglegted. Surface temperature of the solid sphere everywhere equal to the average value of the temperature reading of the thermocouples below and above the sphere.

The experimental results must be correlated by:

1-The viscosity of air can be calculated from eq.13, where μ_o is the viscosity of the air at 0℃ which equals to 0.017 in centipoises and *n* equals to 0.677 (Perry, 1973):

$$\frac{\mu}{\mu_o} = \left[\frac{T}{273}\right]^n \qquad (13)$$

2- Experimental value of mass transfer coefficients was calculated from eq. 14, in which C_b is equal to zero (Perry, 1973, Prins et al., 1985):

$$N = k_g (C_s - C_b) \qquad (14)$$

3- The correlation for diffusivity of naphthalene vapor in air with temperature is made by eq. 15, where the diffusivity of naphthalene vapor in air at 0℃ was taken equal to 0.0513 cm^2/s and m=1.823(Perry, 1973):

$$\frac{Dv}{Dv_o} = \left[\frac{T}{273}\right]^m \qquad (15)$$

4- Vapor pressure of solid naphthalene is given by equation 16 where P_s in *mHg* and T_s in *K*, for the range of (0-80℃) (Perry, 1973):

$$\log Ps = -\frac{3729.3}{Ts} + 11.450 \qquad (16)$$

5- Values of Sherwood number for mass transfer from the sphere to the bed of fluidized particles were calculated by the eq. 17; in which *f(y)* describes the effect of particles motion on transfer rate, and y is a dimensionless group determined by dimensionless analysis (Perry, 1973):

$$Sh = Sh_e + f(y) \tag{17}$$

6- The value of Sherwood number for mass transfer in empty bed calculated from equ.18, where C_1, C_2 and C_3 are constants and determined from the experimental results in empty bed (Ranz, 1952)

$$Sh_e = 2 + C_1 \mathrm{Re}_p^{c_2} Sc^{c_3} \tag{18}$$

Equation 18 for *mass transfer in empty bed* was fitted for air flow through fluidized bed, by assuming the limiting value of Sherwood number, at zero Reynolds number, is equal to 2 because it agrees with the theoretical approach. The experimental results were correlated by using statistical fitting, as shown below:

$$Sh_e = 2 + 0.657 \mathrm{Re}_p^{1/2} Sc^{1/3} \tag{19}$$

With correlation coefficient of 0.9907 and percentage of average errors of 0.62%.

For experiments that carried out at ***minimum fluidizing velocity***, the value of the dimensionless group, Y, is inconsistent with other experiments due to the term (G-G_{mf}) which is equal to zero at minimum fluidizing velocity, so results obtained at minimum fluidization are neglected. The term $f(y)$ in equation 17 is chosen as a power function of Y , that is:

$$f(y) = C_1 y^{C_2} \tag{20}$$

Two attempts have been made to correlate the experimental results:

1. The first attempt was made by choosing the dimensionless function, Y, as given by Ziegler (Ziegler and Holmes, 1966), i.e.:

$$Sh = Sh_e + C_1 \left[\frac{(G - G_{mf})\mu}{(\psi d_p)^2 (\rho_p - \rho)\rho g}\right]^{C_2} \tag{21}$$

   Eq. 21 was fitted for air flow through fluidized bed using the experimental results at minimum fluidization velocity, and was correlated by the following equation:

$$sh = sh_e + 9.6\left(\frac{\mu\left(G - G_{mf}\right)}{\left(\psi d_p\right)^2 \left(\rho_p - \rho\right)\rho g}\right)^{0.014} \tag{22}$$

   With the correlation coefficient of 0.976 and percentage of average errors of 1.57%. **Fig. 7** shows a comparison of eq. 22 with the experimental data. It can be seen from this figure, that the correlation suggested by Ziegler and Holmes don't fit the experimental results of this work.

2. The second attempt was made by taking the dimensionless group, Y , as obtained from the dimensionless analysis, i.e.:

$$Sh = Sh_e + C_1 \left[\frac{(\rho_p - \rho)\rho g (\psi d_p)}{(G - G_{mf})^2}\right]^{C_2} \left[\frac{(\psi d_p)(G - G_{mf})}{\mu}\right]^{C_3} \tag{23}$$

Eq. 23 was fitted using statistical fitting for the experimental results of air flow through fluidized bed at minimum fluidization velocity, the constants of the equation C_1, C_2 and C_3 have been found to be equal to 16.8574, 0.07497 and 0.1284 respectively. With the correlation coefficient of 0.914 and percentage of average errors of 1.544 %. **Fig. 8** shows comparison of eq. 51 with the experimental data. From this

figure it can be notice that this correlation shows a better agreement with experiments, in which 97% of the points have an error less than 25%, consequently this correlation obtained from the present work.

Comparison of Experimental Results with Previous Works and Model

Solid mass capacity has an essential affect on surface-to-fluidized bed mass transfer. For (C_{ms}=0) low mass transfer coefficients are attained and there is no similarity with surface-to-bed heat exchange. In the case of non-zero solid mass capacity, mass transfer coefficients are greater and for small values of (C_{ms}) they may be predicted from the theory proposed by Yokota (Yokota, 1975). For relatively large values of ($C_{ms}d_s^2/\overline{\tau_p}$) greater than 10^{-5} m^2/s the contact resistance is dominant and the surface-to-packet mass transfer coefficient is inversely proportional to (d_s). For small values of $C_{ms}d_s^2/\overline{\tau_p}$ less than 10^{-10} m^2/s the packet resistance predominates and the surface-to-packet mass transfer coefficient is independent of particle size as represented in **Table 6**.

Fig. 9 show a comparison between the experimental results of mass transfer and those obtained from documented experimental literatures data; this comparison are represented in Yokota's coordinate. For very large mass capacities, Sherwood numbers predicted from Yokota's theory considerably overestimate experimental ones, so there must be an additional mass transfer resistance. It is apparent that this resistance depends on particle size and rises as (d_s) increases, which agrees with the contact resistance concept and don't show any appreciable (d_s) dependence.

Studying the Variables Affecting Mass Transfer Coefficient:

Many variables effect mass transfer have been investigated such as: air velocity, sphere surface temperature, size of fluidizing particles and sphere size. The range of sphere surface temperature varied from ambient temperature to a temperature below the melting point of naphthalene. **Figs. 10** and **11** show the effect of air temperature on Sherwood number, **Fig. 12** shows the effect of air flow rate on Sherwood number, **Figs. 13**, **14** and **15** show the effects of both air temperature and particle size on Sherwood number, the effects of both air flow rate and particle size on Sherwood number are showed in **Figs. 16**, **17** and **18** the effects of both particle size and different temperature on Sherwood number are showed in **Figs. 19**, **20**, **21** and **22**.

Conclusions:

In this work, a mathematical model for mass transfer was introduced depends on one dimensionless group which results from the merge of the two dimensionless groups derived in this work and was fitted for air flow through fluidized bed using the experimental results at minimum fluidization velocity. The mathematical model had successfully describes the effects of different parameters on the mass transfer coefficient such as air velocity, sphere surface temperature, size of fluidizing particles and sphere size, when compared with the experimental results and gives a good improvement rather than Ziegler equation.

Sherwood number increased slowly with the increase in gas velocity at constant surface temperature and particle size, although it is increasing with decreasing surface temperature of the sphere at constant U/U_{mf} and particle size, and Sherwood number increased with decreasing particle size at constant U/U_{mf} and temperature.

The ratio of Sherwood number for mass transfer in the presence of solid particles (fluidized bed) to that in absence of solid particles (empty bed) was found to be varied up to 30.

References:

1. Baeyens J. and Geldart D., 1974, "An Investigation into Slugging Fluidized Beds", Chem. Eng. Sci. Vol. 29, pp. 255.

2. Baskakov A. P. and Suprun V. M., 1970, “Mass transfer from a freely moving single sphere to the dense phase of a gas fluidized bed of inert particles”. Sov. Chem. Ind. Vol. 9, pp. 61.

3. Baskakov A. P., 1974, “Critique of the modified packet theory”. Journal of Engineering Physics and Thermophysics, Vol. 28, No. 5, pp. 584-586.

4. Baskakov A. P., B.V. Berg, O.K. Vitt, N.F. Filippovsky, V.A. Kirakosyan, J.M. Goldobin and V.K. Maskaev, (1973), “Heat transfer to objects immersed in fluidized beds”. Powder Technology, Vol. 8, pp. 273-282.

5. Baskakov, A. P. and Suprun V. M., 1972, "The determination of the convective component of the coefficient of heat transfers to a gas in a fluidized bed". Int. Chem. Eng., Vol. 12, pp. 53.

6. Buckingham, Edgar, 1914, "On Physically Similar Systems: Illustrations of the Use of Dimensional Analysis". Phys. Rev. Vol. 4, pp. 345.

7. Gamson B.W., 1951, “Heat and mass transfer in fluidized and packed beds”, Chem. Eng. Progress, vol. 74, no. 1, pp. 19-28.

8. Gunn D. J., 1987, "Axial and Radial Dispersion in Fixed Bed ". Eng. Sci., Vol. 42, pp. 363-373.

9. Gupta C.K. and Sathiyamoorthy D., 1999, "Fluid Bed Technology in Material Processing". CRC Press, Florida, pp. 38.

10. Gupta, A.S. and Thodas, G., 1962, “Liquid-phase mass transfer in fixed and fluidized beds of large particles”. A.I.Ch.Eng., Journal, Vol. 20, No. 1, pp. 20–26.

11. Kafui K.D., Thornton C. and Adams M.J., 2002, "Discrete-Continuum Fluid Modeling of Gas-Solid Fluidized Beds", Chemical Engineering Science, Vol. 57, pp. 2395-2410.

12. Kaneko Y., Shiojima T., and Horio M., 1999, "DEM Simulation of Fluidized Beds for Gas-Phase Olefin Polymerization", Chemical Engineering Science, Vol.54, No. 24, pp. 5809-5821.

13. Kopec J., 1981, “The Kinetics of a Low-Temperature Drying in a Fluidized Bed”. Ph. D. Thesis, Warsaw Technical University.

14. Leva M., Weinfraub M., Grummer M., Pollchik M. and Storch H. H., "Fluid Flow through Packed and Fluidized Systems". U. S. Bureau of Mines Bulltin, 504(1951).

15. Markova M. N. and Martyushin I. G., 1965."An investigation of mass transfer during the vaporization of water from the surface of objects immersed in a fluidized bed of finely divided particles", Chem. Eng. Vol.5, pp. 20-22.

16. Pécora A. A. B. and Parise M. R., 2006, “An Analysis of Process Heat Recovery in a Gas-Solid Shallow Fluidized Bed”. Brazilian Journal of Chemical Engineerin,g Vol. 23, No. 04, pp. 497 - 506.

17. Perry R.H. and Chiton C.H., 1973, Chemical Engineers Handbook. (5th Edition). McGraw-Hill, New York, NY.

18. Prins W., Casteleijn T. P., Draijer W. and. Van Swaaij W. P. M, 1985,” Mass transfer from a freely moving single sphere to the dense phase of a gas fluidized bed of inert particles”. Chem. Eng. Sci., Vol. 40, No. 3, pp. 481-497

19. Prozorov E. N., 1976, “kinetics of the removal of liquid from capillary porous bodies in a fluidized bed under nonisothermal conditions”. Izuest. VUZ-ov Khim. Technol., Vol. 30, No. 6, pp. 1127–1137.

20. Ranz W. E. and Marshall W. R., 1952, "Evaporation from Drops". Chem. Eng. Prog. Vol. 48, pp. 141-173.

21. Resnick W. and White R. R., 1949, “Mass transfer in systems of gas and fluidized solids”. Chem. Eng. Prog. Vol. 45, pp. 377.

22. Rhode, M.J., Wang X.S., Nguyen M., Stewart P., and Liffman K. (2001),"Use of discrete element method simulation in studying fluidization characteristic: influence of antiparticle force", Chemical Engineering Science, Vol. 56. p. 69.

23. Schmidt A., Renz U., 2005, “Numerical prediction of heat transfer between a bubbling fluidized bed and an immersed tube bundle”, Heat-Mass Transfer, Vol. 41, pp. 257–270.

24. Shirai, T., Yoshitome, H. and Shoji Y., 1966, “Heat and Mass transfer on the Surface of Solid Spheres Fixed within Fluidized”. Kagaku Kogaku, Vol. 4, pp. 880 – 884

25. Wankhede U. S., 2009, “Effect of Increase in Surface Temperature on Heat Transfer in a Sound Assisted Fluidized Bed of Fine Powders”. International Journal of Engineering Studies, Vol. 1, No. 1, pp. 31–38.

26. Wen Y.C. and Yu Y.H., 1966, “Mechanics of Fluidization”, Chemical Engineering Progress Symposium Series, Vol. 62, pp. 100-111.

27. Yokota T., Hidaka Y. and Yasutomi T., 1975, “Mass transfere”, Kagaku Kogaku Ronbunshu, Vol.1, p. 399.

28. Ziegler, E. N. and Holmes J. T., 1966,” Mass transfer from fixed surfaces to gas fluidized beds”. Chem. Eng. Sci., Vol. 21, pp. 117-118.

Table 1: Property of Sand Particles

Range of Particle Size (*micron*)	Range Particle Size (*micron*)	Particle Density (Kg/m^3)
75-150	112.5	2600
150-180	165	2600
180-250	215	2600

Table 2: Operational conditions for experiment of mass transfer in empty bed without naphthalene

	Test 1 For sphere of diameter 2.9 cm and weight 8 gm, air flow rate 2.8 m^3/hr, ambient temperature 39^0C, pressure drop 0.9 cm H_2O				Test 2 For sphere of diameter 2.9 cm and weight 8 gm, air flow rate 2.8 m^3/hr, ambient temperature 39.1^0C, pressure drop 0.9 cm H_2O				Test 3 For sphere of diameter 2.9 cm and weight 8 gm, air flow rate 3.7 m^3/hr, ambient temperature 39.1^0C, pressure drop 1.4 cm H_2O			
Time (min)	Wt. Loss (gm)	T_2(°C)	T_1(°C)	Wt.(gm)	Wt. Loss (gm)	T_2(°C)	T_1(°C)	Wt.(gm)	Wt. Loss(gm)	T_2(°C)	T_1(°C)	Wt.(gm)
0	-	39.0	39.0	10.21	-	51.3	51.3	10.2	-	66.0	66.0	12.45
5	0.087	39.1	39.1	10.12	0.2884	51.1	51.2	9.93	1.0717	66.1	66.2	11.38
10	0.079	39.1	39.0	10.04	0.2514	51.3	51.4	9.68	1.0215	66.1	66.2	10.36
15	0.072	39.0	39.0	9.968	0.3102	51.3	51.4	9.37	0.7172	66.1	66.0	9.637
20	0.083	39.0	39.1	9.884	0.1913	51.2	51.2	9.17	0.6251	66.0	66.1	9.013
25	0.079	39.0	39.0	9.805	0.1241	51.1	51.3	9.05	0.6765	66.1	66.0	8.337

Note: T_1 = Temperature below the sphere, T_2 = Temperature above the sphere.

Table 3: Operational conditions for experiment of mass transfer in fluidized bed without naphthalene

Tests	Test 1 for sphere of diameter 2.9 cm and weight 8 gm, air flow rate 4 m^3/hr, ambient temperature 39^{0}C, pressure drop 21 cm H_2O				Test 2 for sphere of diameter 2.9 cm and weight 8 gm, air flow rate 4.8 m^3/hr, ambient temperature 39.3^{0}C, pressure drop 23 cm H_2O				Test 3 for sphere of diameter 2.9 cm and weight 8 gm, air flow rate 5.2 m^3/hr, ambient temperature 39.4^{0}C, pressure drop 25 cm H_2O			
Time (min)	Wt. Loss(gm)	T_2(℃)	T_1(℃)	Wt.(gm)	Wt. Loss(gm)	T_2(℃)	T_1(℃)	Wt.(gm)	Wt. Loss(gm)	T_2(℃)	T_1(℃)	Wt.(gm)
0	-	39.1	39.1	12.74	-	51.2	51.2	12.35	-	66.1	66.2	15.56
5	0.1147	39.0	39.1	12.63	0.45317	51.0	51.0	11.89	1.5197	66.1	66.1	14.04
10	0.1954	39.0	39.0	12.43	0.48788	51.1	51.2	11.40	1.4178	66.0	66.1	12.63
15	0.1721	39.1	39.2	12.26	0.39927	51.1	51.1	11.01	1.5503	66.1	66.0	11.07
20	0.1229	39.1	39.0	12.13	0.47188	51.0	51.1	10.53	1.2799	66.1	66.3	9.795
25	0.1627	39.2	39.2	11.97	0.5561	51.1	51.0	9.98	1.6998	66.0	66.0	8.095

Table 4: Operational conditions and results for mass transfer in empty bed

Tests no.	Air Flow rate(m^3/hr)	Temp ^0C	Weight Loss ($gm/hr.m^2$)	Re_p	Sh_e
1	2.8	39.0	16.0007	285.1003	17.3135
2	3.4	39.1	17.4398	345.8269	18.7098
3	3.7	39.2	18.3160	377.7627	19.3947
4	4.0	39.0	18.4545	406.7856	19.9931
5	4.5	39.1	19.6208	458.6925	21.0113
6	5.2	39.0	20.6403	529.8438	22.3181
7	2.8	51.3	46.3716	277.7204	17.1085
8	2.8	55.3	65.2329	272.8329	16.9799
9	2.8	66.1	148.507	266.4974	16.8026
10	3.4	51.2	49.6271	336.7652	18.4820
11	3.4	55.2	68.0483	330.7357	18.3388
12	3.4	66.1	160.042	323.0021	18.1415
13	3.7	51.2	51.7253	368.4121	19.1685
14	3.7	55.3	71.6804	362.3935	19.0308
15	3.7	66.0	163.612	350.6095	18.7530
16	4.0	51.1	52.5007	396.0089	19.7436
17	4.0	55.3	73.0415	388.2574	19.5742
18	4.0	66.2	171.623	378.8475	19.3535
19	4.5	51.3	56.4473	447.5064	20.7647
20	4.5	55.3	77.5178	440.0929	20.6113
21	4.5	66.2	179.185	424.9063	20.2874
22	5.2	51.2	59.3788	516.9524	22.0536
23	5.2	55.3	82.1496	507.9866	21.8811
24	5.2	66.2	189.438	489.2557	21.5112

*Air flow rate measured at ambient temperature.

Table 5: Experimental conditions for mass transfer in fluidized bed

Sand Mean Particle Size (*micron*)	Exp. No.	Air Flow Rate (m^3/hr)	U/U_{mf}	Temp. ^0C	Wt. Loss ($gm/hr.m^2$)	Re_p	Sh_e
215	1	4.0	1.081	39.1	30.550	943.71	254.612
	2	4.4	1.189	39.1	31.754	964.75	258.791
	3	4.8	1.297	39.2	33.483	972.29	262.413
	4	5.2	1.405	39.2	34.911	982.71	269.751
	5	4.0	1.081	51.0	84.836	951.64	214.622
	6	4.4	1.189	51.0	89.614	967.90	225.704
	7	4.8	1.297	51.2	94.233	971.53	243.950
	8	5.2	1.405	51.3	98.408	979.46	257.568
	٩	4.0	1.081	55.2	121.607	916.60	203.815
	10	4.4	1.189	55.1	124.457	945.03	217.780
	11	4.8	1.297	55.2	130.413	969.87	247.502
	12	5.2	1.405	55.0	132.781	972.37	227.235
	13	4.0	1.081	66.3	285.096	884.27	172.751
	14	4.4	1.189	66.1	295.131	989.40	194.224
	15	4.8	1.297	66.0	297.444	944.85	203.705

	16	5.2	1.405	66.3	313.011	961.19	214.443
165	1	3.0	1.071	39.0	25.509	661.73	281.599
	2	3.4	1.214	39.0	27.221	753.69	305.431
	3	3.8	1.714	39.2	29.075	839.76	334.890
	4	4.0	1.428	39.1	29.756	889.36	344.508
	5	3.0	1.071	51.1	73.244	648.80	264.114
	6	3.4	1.214	51.3	78.891	734.67	283.170
	7	3.8	1.714	51.0	81.180	822.97	295.800
	8	4.0	1.428	51.1	84.641	871.43	307.709
	9	3.0	1.071	55.0	100.240	640.28	247.105
	10	3.4	1.214	55.1	107.812	728.69	265.401
	11	3.8	1.714	55.3	115.400	814.63	281.715
	12	4.0	1.428	55.2	117.142	857.09	299.552
	13	3.0	1.071	66.0	240.074	629.50	227.746
	14	3.4	1.214	66.1	256.227	713.26	239.534
	15	3.8	1.714	66.2	270.089	782.94	252.753
	16	4.0	1.428	66.3	280.120	827.04	274.766
112.5	1	2.4	1.091	39.0	23.162	524.39	349.553
	2	2.8	1.272	39.1	25.077	611.68	364.710
	3	3.0	1.363	39.2	25.833	650.19	377.455
	4	3.2	1.454	39.0	26.042	692.23	389.107
	5	2.4	1.091	51.1	64.938	505.76	327.114
	6	2.8	1.272	51.2	70.487	591.29	339.415
	7	3.0	1.363	51.3	74.378	639.27	359.770
	8	3.2	1.454	51.0	75.018	683.96	378.105
	9	2.4	1.091	55.3	91.653	500.88	314.211
	10	2.8	1.272	55.2	99.647	593.28	332.154
	11	3.0	1.363	55.1	100.780	630.22	351.005
	12	3.2	1.454	55.0	103.917	676.43	368.417
	13	2.4	1.091	66.0	212.427	489.99	305.215
	14	2.8	1.272	66.1	230.876	573.56	319.419
	15	3.0	1.363	66.3	682.796	930.62	335.498
	16	3.2	1.454	66.2	698.345	992.66	357.794

Table 6: Comparison of the orders of magnitude of the experimental parameters

	Silica gel-air-water ($R_{mp}/R_{mw} \sim 0$)	Sand-air-water ($R_{mp}/R_{mw} \sim \infty$)	Sand-air-naphthalene ($R_{mp}/R_{mw} \sim \infty$)
$D_f \rho_s / \beta \rho_f$ (m^2/s)	10^{-3}	10^{-2}	10^{-2}
$\bar{C}_m / C_{ms}$	10^{2}	10^{2}	10^{3}
$d_s^2 C_{ms} / \bar{\tau}_p$ (m^2/s)	10^{-5},10^{-6}	10^{-11},10^{-12}	10^{-9},10^{-10}

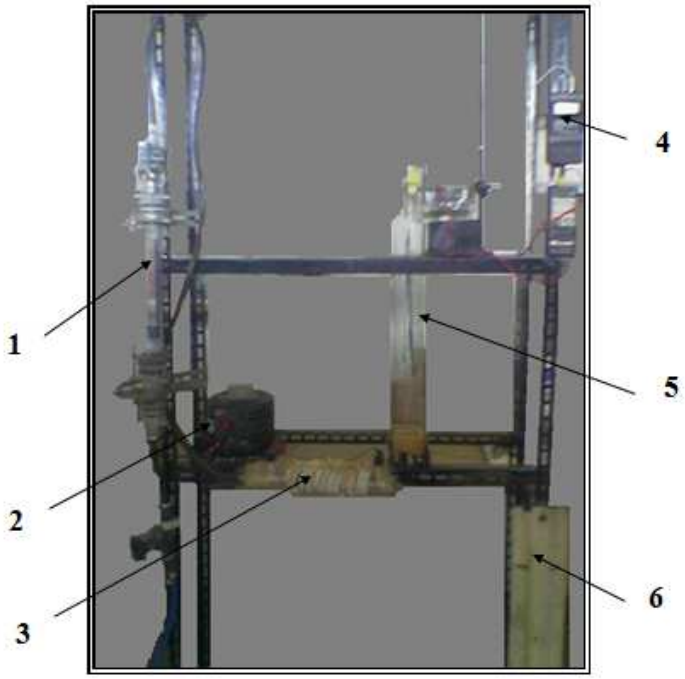

1. Rotameter
2. Variac
3. Heating Equipment
4. Temperature Reader
5. Fluidization Column
6. Manometer

Fig. 1: Photographic picture of the Experimental Equipment

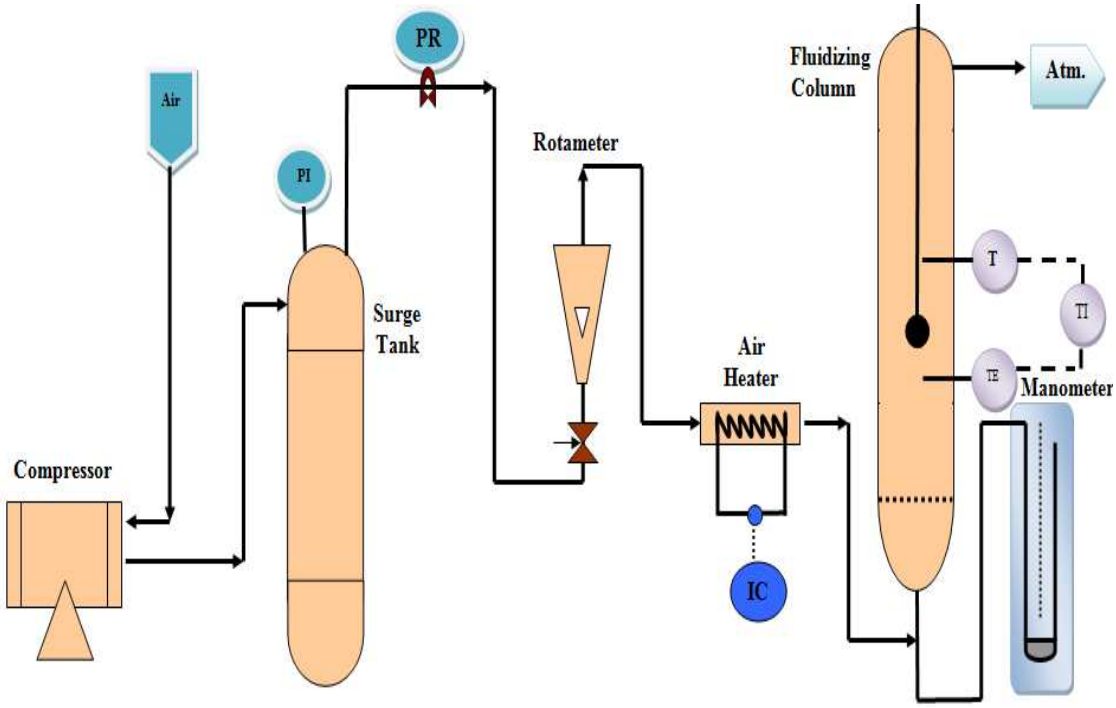

Fig. 2: Experimental setup.

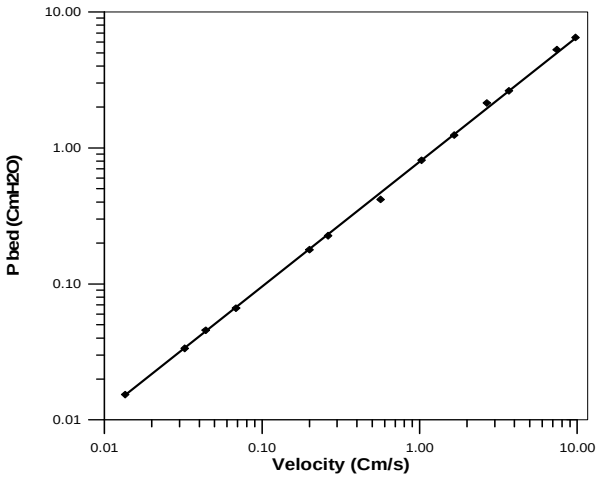

Fig. 3: Distributor Pressure Drop

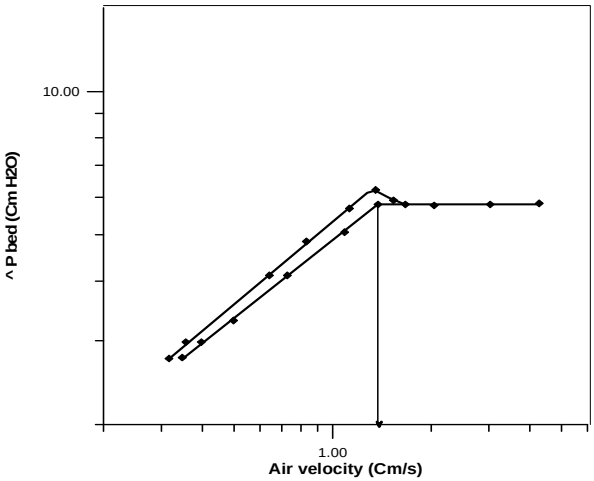

Fig. 4: Bed Pressure Drop vs. Air Velocity (Sand Particle Size = 215 Micron)

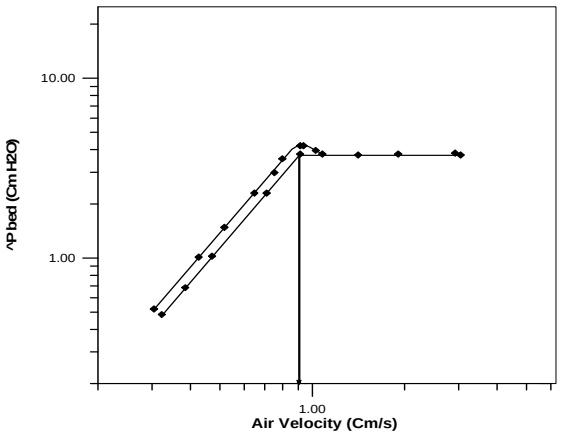

Fig. 5: Bed Pressure Drop vs. Air Velocity (Sand Particle Size = 165 Micron)

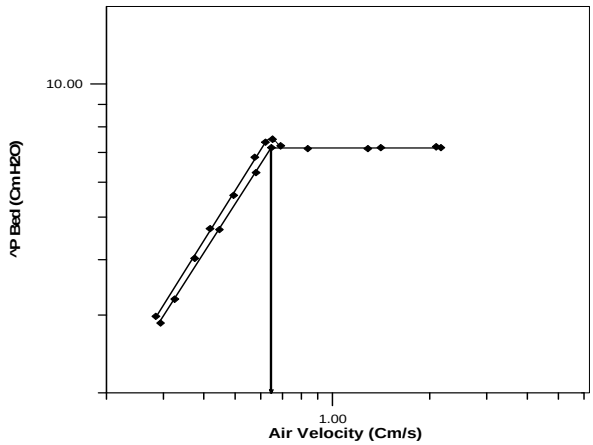

Fig. 6: Bed Pressure Drop vs. Air Velocity (Sand Particle Size= 112.5 Micron)

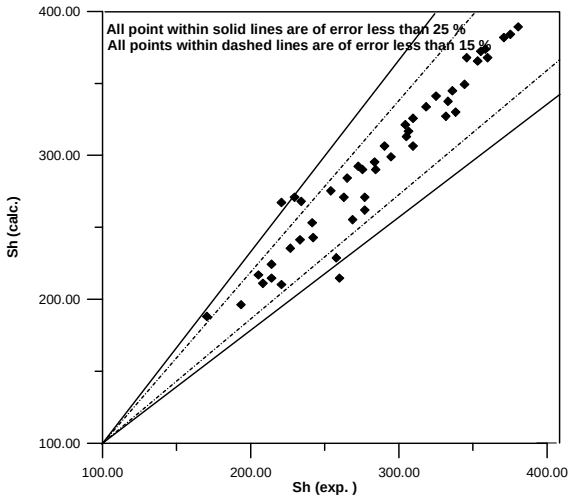

Fig. 7: A comparison of eq. 50 with the experimental data

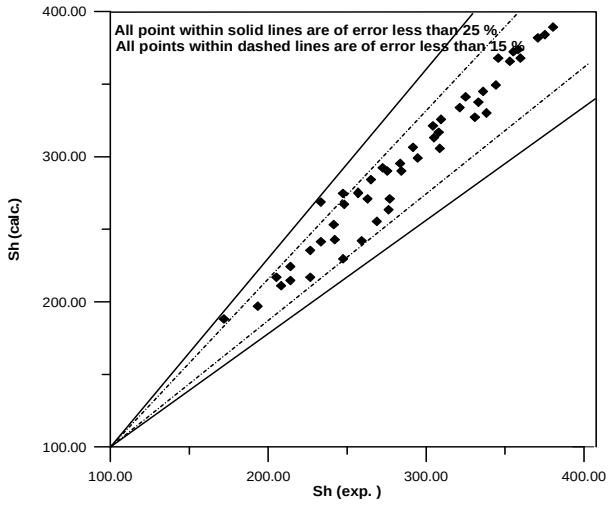

Fig. 8: A comparison of eq. 51 with the experimental data

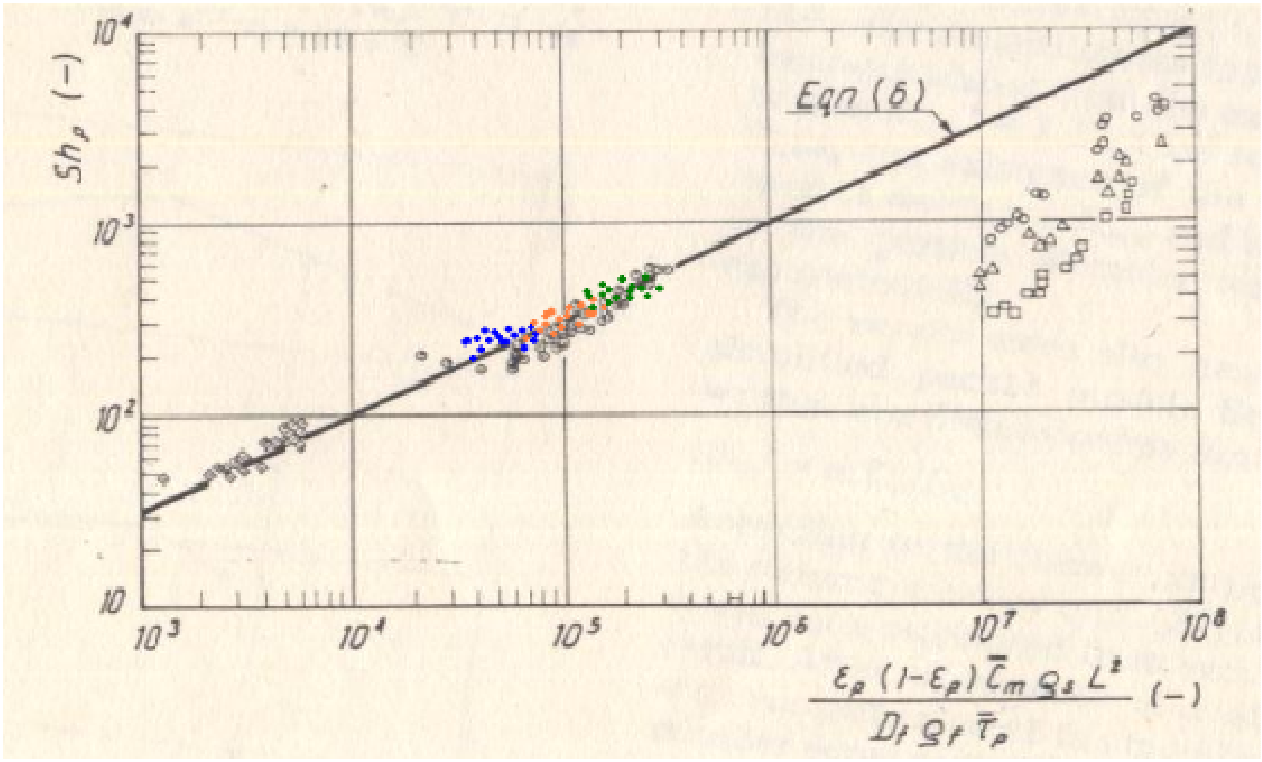

Fig. 9: Comparison of Experimental Data with The Packet Theory Systems is follows:
Silica gel-air-water [(o) d_s=0.548mm, (△) d_s=0.875 mm, (□) d_s=1.342mm].
Sand-air-water [(◊) d_s=0.496mm].Sand-air-naphthalene [(□)d_s=0.351mm] (Yokota, 1975).
Sand-air-naphthalene (present work) [(▪) ds=215 micron, (▪) ds=165 micron, (▪) d_s= 112.5 micron]

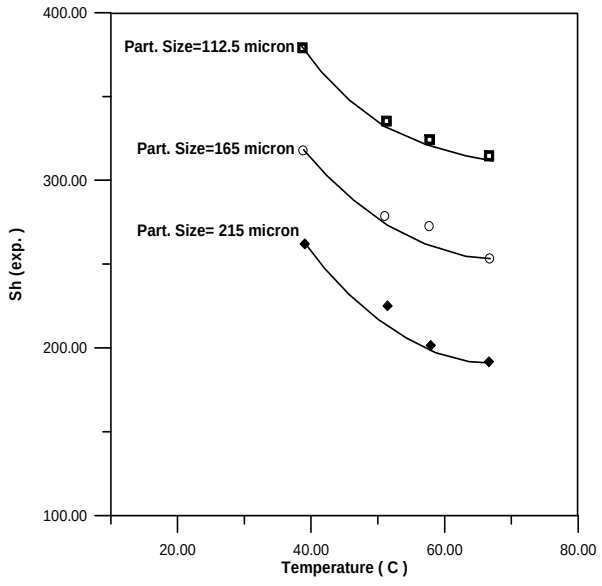

Fig. 10: Experimental Sh. vs. Temperature at Air Flow Rate = 1.2 Umf

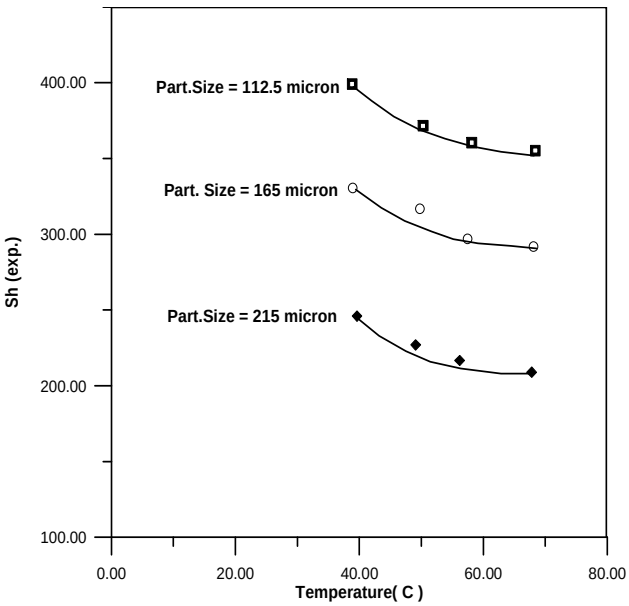

Fig. 11: Experimental Sh. vs. Temperature at Air Flow Rate = 1.4 Umf

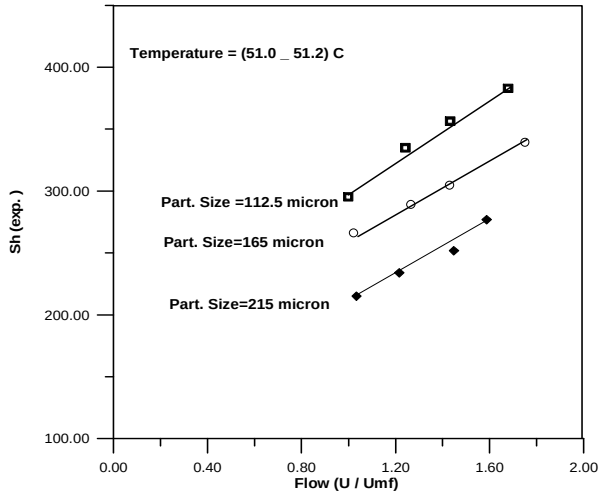

Fig. 12: Experimental Sh. vs. Air Flow Rate

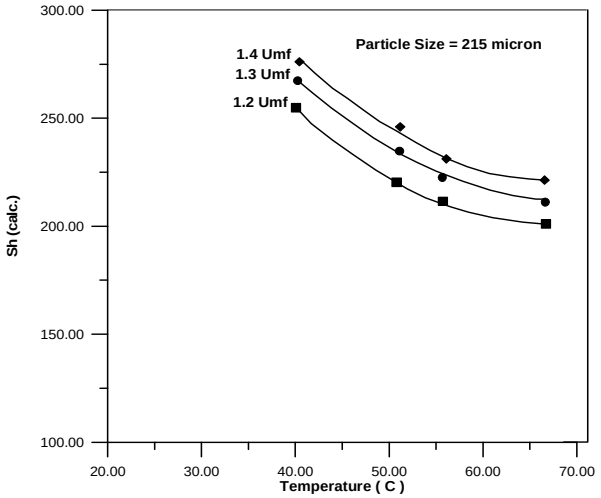

Fig. 13: Effect of Temperature on Calculated Sh. No

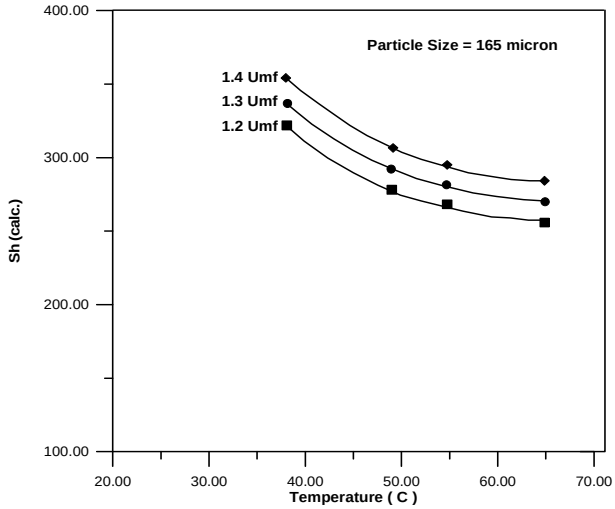

Fig. 14: Effect of Temperature on Calculated Sh No.

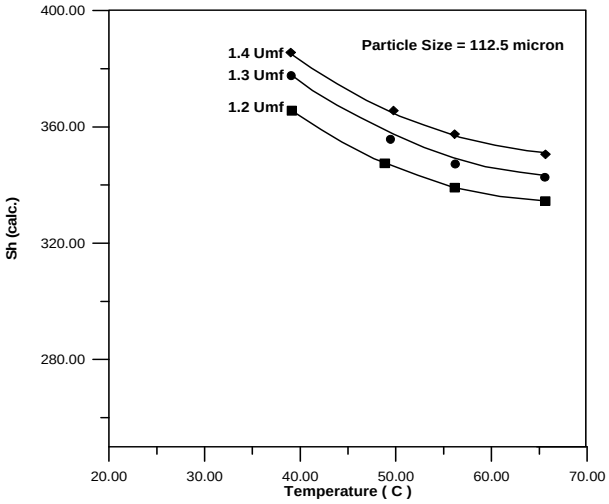

Fig. 15: Effect of Temperature on Calculated Sh. No.

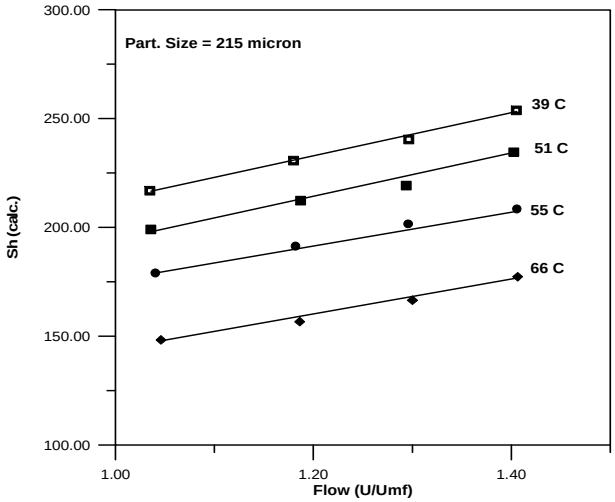

Fig. 16: Effect of Air Flow Rate on Calculated Sh. No.

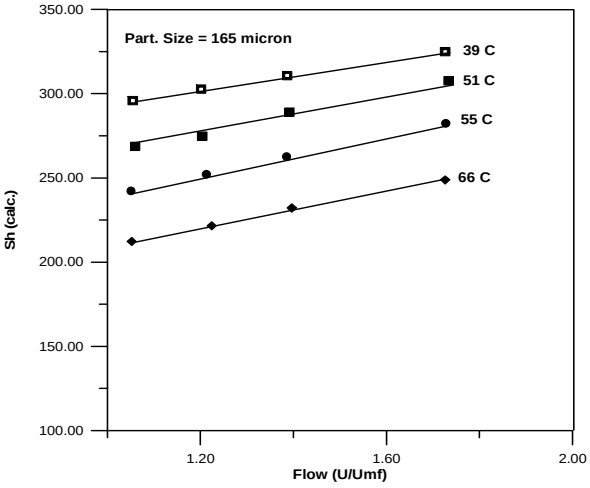

Fig. 17: Effect of Air Flow Rate on Calculated Sh. No.

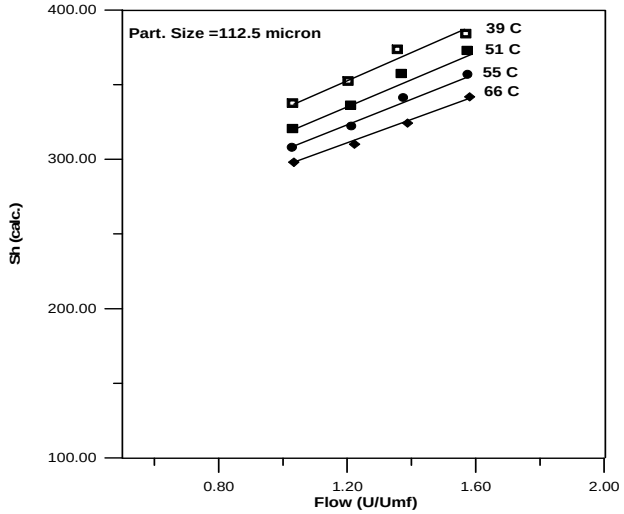

Fig. 18: Effect of Air Flow Rate on Calculated Sh. No.

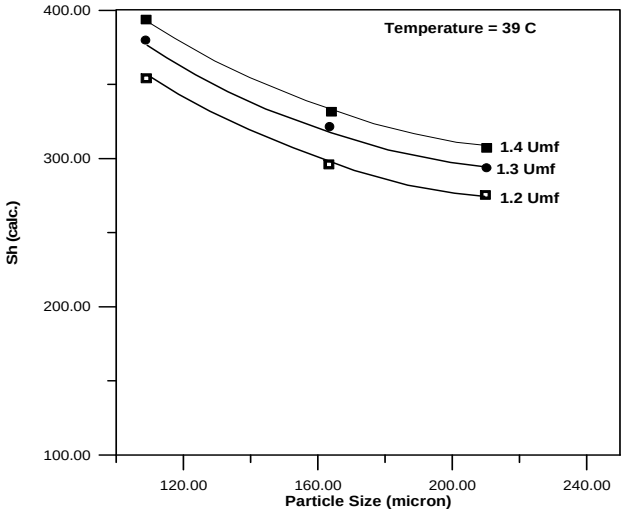

Fig. 19: Effect of Sand Particle Size on Calculated Sh. No

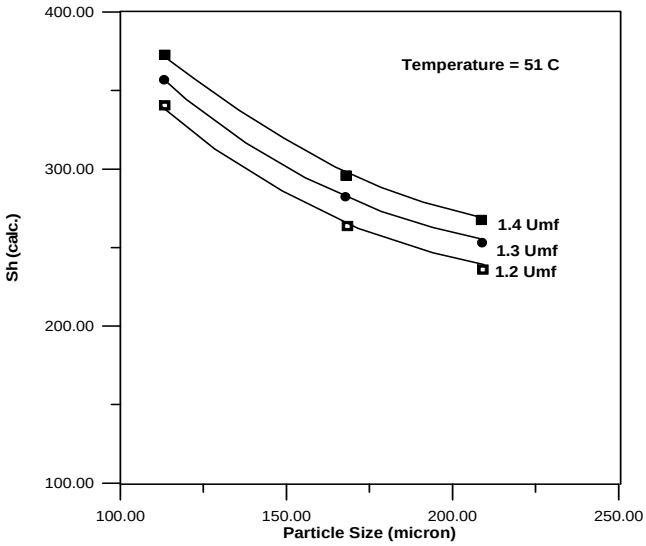

Fig. 20: Effect of Sand Particle Size on Calculated Sh. No.

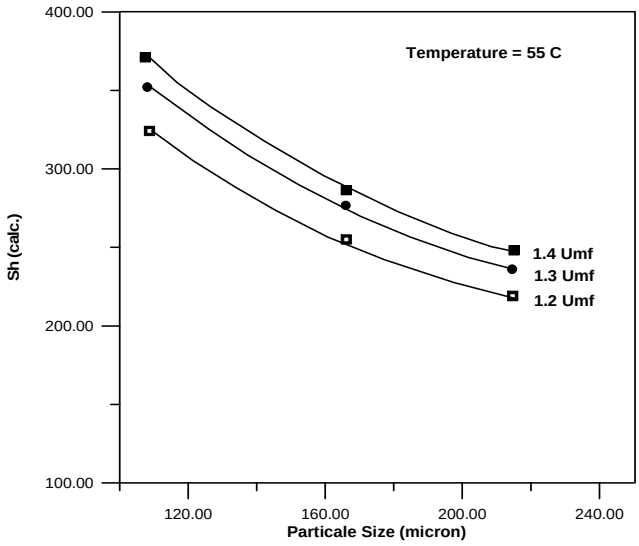

Fig. 21: Effect of Sand Particle Size on Calculated Sh. No

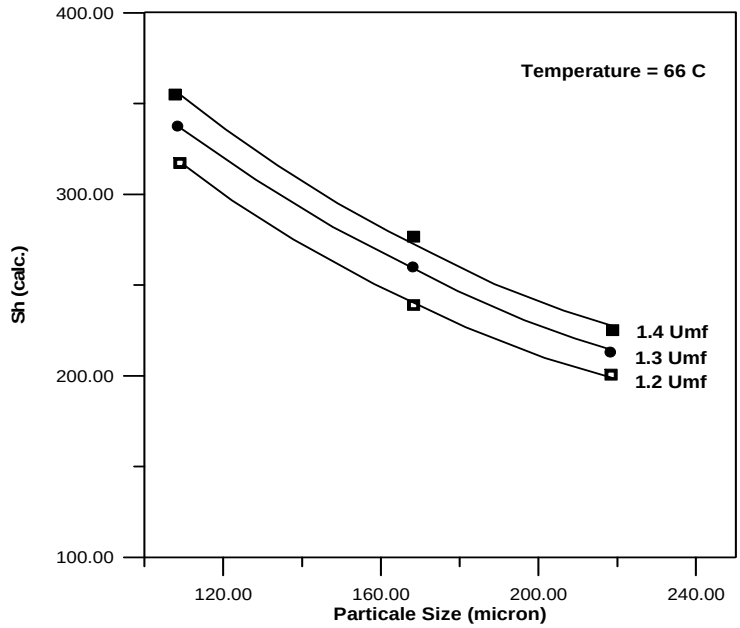

Fig. 22: Effect of Sand Particle Size on Calculated Sh. No.